Ginkgolide B Exerts Cardioprotective Properties against Doxorubicin-Induced Cardiotoxicity by Regulating Reactive Oxygen Species, Akt and Calcium Signaling Pathways *In Vitro* and *In Vivo*

Junqing Gao[�}, **Tao Chen**[�}, **Deqiang Zhao, Jianpu Zheng** *, **Zongjun Liu** *

Department of Cardiology, Putuo Hospital, Shanghai University of Traditional Chinese Medicine, Shanghai, People's Republic of China

☺ These authors contributed equally to this work.
* liuzongjun028@sina.com (JZ); zhengjianpu_p@163.com (ZL)

Abstract

The aim of this study was to evaluate the effect of Ginkgolide B (GB) on doxorubicin (DOX) induced cardiotoxicity *in vitro* and *in vivo*. Rat cardiomyocyte cell line H9c2 was pretreated with GB and subsequently subjected to doxorubicin treatment. Cell viability and cell apoptosis were assessed by MTT assay and Hoechst staining, respectively. Reactive oxygen species (ROS), Akt phosphorylation and intracellular calcium were equally determined in order to explore the underlying molecular mechanism. To verify the *in vivo* therapeutic effect of GB, we established a mouse model of cardiotoxicity and determined left ventricle ejection fraction (LVEF) and left ventricular mass (LVM). The *in vitro* experimental results indicated that pretreatment with GB significantly decreases the viability and apoptosis of H9c2 cells by decreasing ROS and intracellular calcium levels and activating Akt phosphorylation. In the *in vivo* study, we recorded an improved LVEF and a decreased LVM in the group of cardiotoxic rats treated with GB. Altogether, our findings anticipate that GB exerts a cardioprotective effect through possible regulation of the ROS, Akt and calcium pathways. The findings suggest that combination of GB with DOX in chemotherapy could help avoid the cardiotoxic side effects of GB.

Introduction

Doxorubicin (DOX), a potent anthracycline antibiotic, is widely recognized as an effective chemotherapeutic agent used in the therapy of different types of cancer in clinical settings [1–9]. However, regrettably, several studies have reported that DOX induces dose-dependent acute or chronic cardiotoxicity [10–15] through a variety of mechanisms involving increased cardiac oxidative stress, changes in adenylate cyclase activity, lipid peroxidation, and the activation of inflammation and apoptosis-related signaling pathways [16, 17], leading to late-onset

cardiomyopathy in a dose cumulative manner [18].These cardiotoxic effects constitute a key drawback of DOX-based chemotherapy [19].

Due to the relevance and the efficacy of DOX in cancer chemotherapy, strategies for preventing or attenuating the side effects of DOX administration, including the alternative drugs with antagonistic properties against DOX induced cardiotoxicity, nanoparticle co-delivery system, and the iron-chelating agents [20–29] have been attempted. Nevertheless, definitively efficient drugs to against DOX-cardiotoxicity have not been developed so far and the discovery of novel agents for thwarting its side effects is still encouraged.

In recent years, numerous research works have indicated that extracts of *Ginkgo biloba* leaves may be beneficial for preventing from the drug-induced toxicity on non-tumour tissues such as the liver, lung, kidney, and heart due to its various pharmacological properties, including anti-inflammatory effect, anti-tumor effect, anti-apoptotic effect, and antioxidant activity [30–35].

Ginkgolide B (GB) is the major terpenoid component extracted from *G. Biloba* leaves. Previous studies have suggested that GB could exert an antagonistic activity against the platelet activating factor (PAF) to subsequently inhibit PAF-induced cascade effect in inflammatory reactions [36–38]. Most recently, researchers have discovered that GB exerts modulatory or protective functions by reducing oxidative stress and Aβ-induced dysfunction of mitochondrial oxidative phosphorylation of the neuronal cells and maintaining cellular energy demands [39]. However, surveys on the effect of GB on DOX-induced cardiotoxicity and the potential molecular mechanisms are limited and need an in-depth elucidation.

Thus, the present study was designed to examine the potential protective effect of GB against DOX-induced cardiotoxicity and to give insights into its possible underlying molecular mechanisms. Specifically, we studied the effect of GB pretreatment on the viability of cardiomyocytes challenged with DOX *in vitro* and its cardio-protective effects *in vivo* and found that GB could protect against DOX induced cell death in H9c2 cardiomyocytes and improved cardiac function *in vivo*.

Methods

Cell culture

Rat H9c2 cells were purchased from American Type Culture Collection (ATCC, Manassas, VA) and cultured in high-glucose DMEM media containing 10% fetal bovine serum (FBS), 100 U/ml penicillin and 100 μg/ml streptomycin. Cells were cultured in a 5% CO_2 incubator at 37°C and were split when 80% confluence was reached.

Cell viability assay

Cardiomyocytes (4×10^3 cells) were suspended in 100 μL culture media and seeded in triplicate in 96-well plate overnight. Thereafter, cell cultures were incubated with a series of different concentrations (0–10 μM) of DOX (Sigma-Aldrich Co.Ltd; St. Louis, MO, USA) for 72 h in the presence or absence of indicated concentrations (0–100 mM; dissolved in DMSO) of GB (sc-201037, Santa Cruz Biotechnology, Santa Cruz, CA) for 24 h. The purity of GB was more than 90%. In the setting of verification of the protective role of GB, cardiomyocytes were either pretreated with 1, 5 and 50 μM GB for 30 min before being challenged with 5 μM DOX or treated with 5 μM DOX 3 h before incubating with 1, 5 and 50 μM GB. In the investigation of molecular mechanisms, cardiomyocytes were pretreated with 50 μM GB or small molecular inhibitors targeting given metabolic pathways (LY294002 (10 μM) or KN62 (10 μM)) for 30 min before being challenged with 5 μM DOX. After 48 h incubation, 3-(4,5-dimethylthiazolyl-2)-2,5-diphenyltetrazolium bromide (MTT: 0.5 mg/ml; Sigma, MO, USA)[40–42] was added

and further incubated for 4 h, followed by addition of formazan dye dissolved with DMSO in a microplate reader (Biotek Instruments, Winooski, VT) and reading at 570 nm. Cell viability expressed as relative viability compared with control in each experiment. All the experiments were performed in triplicate.

Hoechst nuclear staining

Double nuclear staining with fluorescent dyes Hoechst 33258 (Beyotime, Nantong, China) was used to determined cell apoptosis according to a previous protocol [43]. Briefly, after the cells were incubated with different treatment for 24 h, Hoechst 33258 was added into the culture medium at a concentration of 8 μM, and incubated at 4°C for 30 min. Images were captured by a confocal microscope and cells in 5 randomly picked fields (400× magnification) were counted, and the percentage of apoptotic cells were calculated.

Annexin V/propidium iodide staining

The H9c2 cardiomyocytes were processed with Annexin V/propidium iodide (PI) staining according to the manufacturer's instructions (Beyotime, Nantong, China). The samples were analyzed by a FACSCalibur flow cytometry (Becton Dickinson, Franklin Lakes, NJ).

Immunofluoresence analysis

After different treatments, cardiomyocytes were fixed with 4% paraformaldehyde. Cells were stained with rat anti phospho-Akt antibody (Cell Signalling Technology) and then with secondary antibody Alexa Fluor® 555 (Invitrogen). Simultaneously, cellular nuclei were stained with 4',6-diamidino-2-phenylindole 4',6-Diamidino-2-phenylindole (DAPI, Molecular Probes, Carlsland, CA). After secondary labelling, cells were washed with PBS and fixed with ProLong® Gold antifade reagent. Fluorescence microscopy was used to determine the fluorescence signals (Olympus, Japan).

Western-blot analysis

Total proteins were extracted from cardiomyocytes as described elsewhere [44], subsequently separated by electrophoresis on SDS-PAGE gel and then transferred onto PVDF membrane. After blocking, the blots were incubated with the antibodies against Caspase-3 (Abcam, Cambridge, MA), phosporylated or total Akt (Millipore, Beverly, MA), p38 (Santa Cruz Technology, Santa Cruz, CA), JNK (Cell signaling Technology, Beverly, MA), Erk (Cell signaling Technology) or CamKII (Cell signaling Technology). β-actin (Abcam) was used as loading control. Following, samples where incubated with appropriate HPR conjugated secondary antibodies. The protein bands were revealed using the SuperSignal Ultra Chemiluminescent Substrate (Pierce, Rockford, IL USA) on X-ray films (Koda, Lexington, MA, USA) followed by data quantification processing using Image J software (NIH, Bethesda, MD, USA).

Assessment of intracellular Ca^{2+}

After the cultured H9c2 cardiomyocytes adhered to the chamber cover-slips, the standard Tyrode's solution (126 mM NaCl, 5.4 mM KCl, 10 mM HEPES, 0.33 mM $NaH_2PO_4 \cdot 2H_2O$, 1.0 mM $MgCl_2 \cdot 6H_2O$, 1.8 mM $CaCl_2$ and 10 mM Glucose; pH = 7.40) was used to rinse cells. Thereafter, cells were incubated with a working solution containing Fura-2/AM (20 mM, Beyotimes, Nantong, China) and Pluronic F-127 (0.03%) at 37°C for 45 min. Once loaded, the above standard Tyrode's solution was used again to wash cells and eliminate the extracellular fluo-3/AM. The concentration of Ca^{2+} was measured using Ca^{2+} indicator fluo-3/AM as

probe. The images were captured using a 20× objective (488 nm excitation, 530 nm emission). Scanning time was 30 min. Reagents were added between the 3rd and 4th scans (10 s interval) and the images were saved.

Detection of reactive oxygen species (ROS)

Cardiomyotes were pretreated with 5 μM GB and incubated with 5 μM DOX for 24 h. After that, ROS was induced by treatment with retigeric acid B (RAB). Subsequently, flow cytometry was employed for detecting ROS using the fluoprobe hydroethidine 2',7'-Dichlorodihydro-fluorescein diacetate (H2DCFDA, Beyotimes, Nantong, China) according to the manufacturer's instructions. Briefly, around 1×10^6 PBS-washed cells of each treatment group were loaded with 0.5 ml PBS containing 10 μM of H2DCFDA and incubated in the darkness for 40 min. The parameter settings for flow cytometry were: emission wavelength = 535 nm, excitation wavelength = 488 nm. The ROS level was proportionally deduced from the fluorescence intensity of the oxidized product of H2DCFDA (2', 7'-dichlorofluorescein).

Animal studies

Ethics statement. The animal study protocol was approved by the institutional animal care and use committee of the Putuo Hospital affiliated to Shanghai University of Traditional Chinese Medicine and was performed in accordance with the generally accepted international guidelines for animal experimentation. The animals were maintained in appropriate cages at 22±1°C on a 12 h light/dark cycle with free access to food and water, and were allowed to acclimatize for a minimum of 1 week before the experiment. Efforts were made to minimize pain by isoflurane anesthesia.

***In vivo* mouse model of DOX-induced cardiotoxicity.** C57BL/10 mice (8- to 10-week-old) were randomly divided into 4 groups (*n* = 6 per group). Two groups received DOX (Santa Cruz Technology; 20 mg/kg; i.p.) at a dose that had been shown to be cardiotoxic [45]. Four days before DOX application, in one DOX group, a treatment with GB (100 mg/kg/day, i.p.; Sigma-Aldrich) was started. The other DOX group received saline. The other two groups without DOX application received no further treatment or the same GB as above. Five days after DOX injection, the Vevo770TM imaging system (VisualSonics Inc., Toronto, Canada) was used to measure mice electrocardiograms (ECGs). The left ventricle ejection fraction (LVEF) was calculated according to a previous protocol [46, 47]. Briefly, mice were put under isoflurane anesthesia and a rectal probe and an infrared heating lamp were respectively used to monitor and control the body temperature. Electrode pads on the heated platform was used to monitor the ECG signal. Chest hair was removed using razor and a chemical depilator to minimize ultrasound attenuation. By using the warm ultrasound gel, we placed the ultrasound probe (RMV-707B) on the chest of the mice. Two-dimensional images were taken in the parasternal short- and long- axis views to direct the M-mode records obtained at the mid-ventricular level, using 3 to 5 measurements for each view and the mean was calculated. The LV systolic function was calculated based on the M-mode measurements following the recommendations of the American Society of Echocardiography Committee. After the echocardiography, all the animals were euthanatized with an overdose of sodium pentobarbital (i.p.).

Statistical analysis

All the statistical analyses were performed using GraphPad Prism software version 6. The data was presented as Mean ± S.E.M. One way-ANOVA was used to examine the difference in three or more groups followed by Tukey's post-hoc test. $P < 0.05$ was considered for statistical significance.

Results

GB protects from DOX-induced cardiac cell death

Prior to the investigation of the effect of GB on DOX-induced cardiotoxicity, we measured the effect of different concentrations of these agents on the viability of rat H9c2 cells in order to determine the optimal concentration of DOX and safety dosage for GB treatment. The results showed that 5 μM DOX could achieve an appropriate degree of cell death after 48 h (Fig 1A) and the viability of cardiomyocytes was not affected up to 50 μM GB (Fig 1B). Thereafter, we employed two models to test the protective effect of GB against DOX cardiotoxicity and found that in the model of cardiomyocytes treatment with DOX for 3 h before GB application, GB treatment did not reverse the toxic effect of DOX on cardiomyocytes (Fig 1C). On the contrary, in the model that cardiomyocytes were pretreated with GB for 30 min before DOX incubation, significantly increased cell viability was observed (Fig 1D). Microscopic examination revealed results similar to that of the MTT assay (Fig 1E).

GB protects from DOX-induced cardiac cell apoptosis

To determine the extent of cell apoptosis, we first performed Hoechst nuclear staining and found that 5 μM GB pretreatment significantly decreased cell death (Fig 2A). Further, Annexin
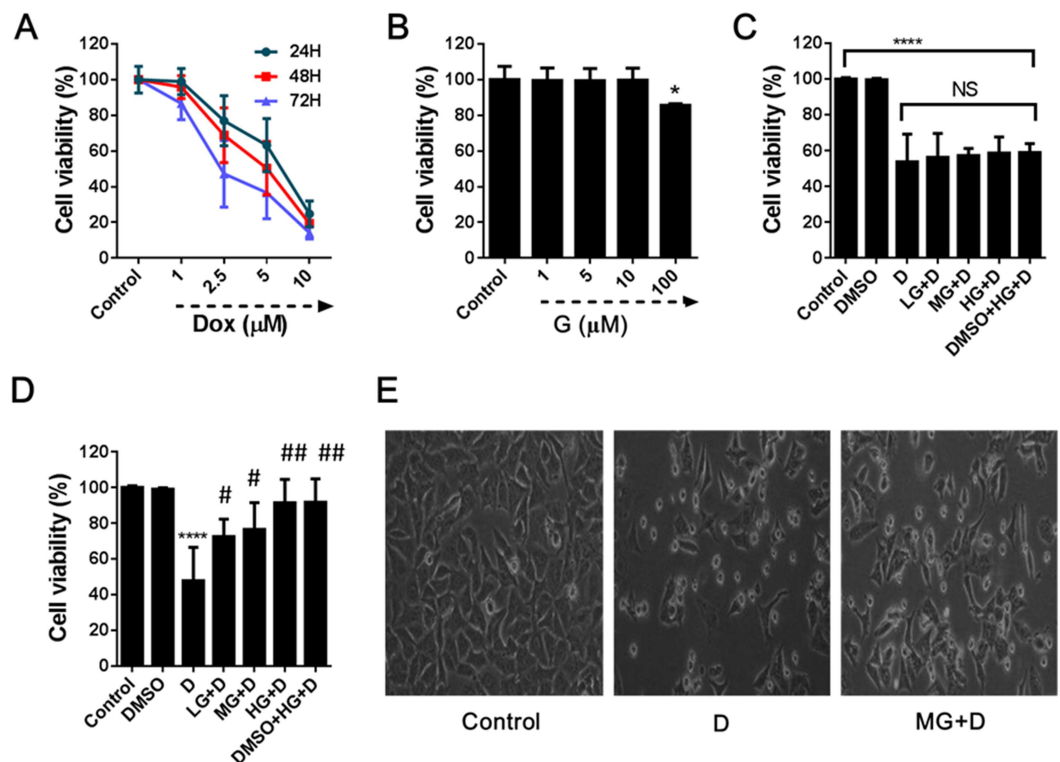

Fig 1. Protective effect of GB against DOX-induced cardiac cell death. (**A**) Time and dose-dependent DOX-induced cardiac cell death was determined by MTT assay. (**B**) The safety dosage of GB on the cardiomyocytes viability was assessed by MTT assay. (**C**) Cardiomyocytes were treated with low (LG, 1μM) medium (MG, 5 μM) and high (HG, 50 μM) of GB after DOX treatment for 3 h and no improvement was found on the cardiomyocytes viability in DOX induced cardiotoxicity. (**D**) Pretreatment with low (LG), medium (MG) and high (HG) doses of GB for 30 min prior to DOX-induced cardiotoxicity increased cardiomyocytes viability. (**E**) Representative images of the effects of DOX and pretreatment with GB for 30 min on cardiomyocytes proliferation. ****p<0.0001 when compared to control group, #p<0.01, ##p<0.001 when compared to DOX.
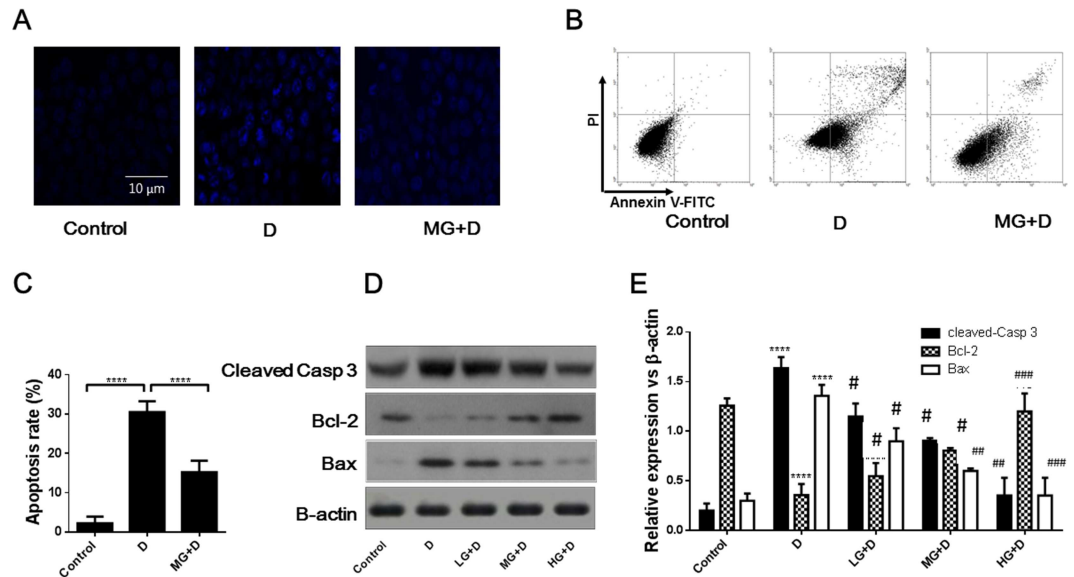
doi:10.1371/journal.pone.0168219.g001

Fig 2. Protective effect of GB against DOX induced cardiomyocytes apoptosis. (A) Representative images of Hoechst nuclear staining in each group. The extent of nuclear damage was decreased in the group of GB pretreatment for 30 min followed by DOX-induced cardiotoxicity comparatively to the DOX group. (B) Flow cytometry analysis of the cardiomyocytes apoptosis. Protective effects of GB pretreatment on the apoptosis of cardiomyocytes were demonstrated by Annexin V/PI staining. (C) Quantitative representation of the flow cytometry analysis. Cardiomyocytes apoptosis was inhibited following GB pretreatment for 30 min before DOX-induced cardiotoxicity. (D) and (E) Western-blot analysis of apoptosis related proteins (cleaved caspase 3, Bcl-2 and Bax) in cardiomyocytes after GB pretreatment for 30 min prior to DOX-induced cardiotoxicity. ****$p<0.0001$ when compared to control group, #$p<0.05$ ##$p<0.01$, ###$p<0.001$ when compared to the DOX group.

doi:10.1371/journal.pone.0168219.g002

V/PI staining indicated that GB pretreatment significantly reduced DOX-induced cardiac cell apoptosis (Fig 2B and 2C). The measurement of the effect of pretreatment with different GB dosages on the expression of apoptotic markers by western blotting showed that GB induces the expression of Bcl-2 and repressed the expression of Bax in a dose-dependent manner (Fig 2C and 2D). The cleaved capase-3 was also evaluated and the results showed that GB pretreatment noticeably decreased the level of cleaved-caspase-3 (Fig 2D), which is indicative of reduced cell apoptosis.
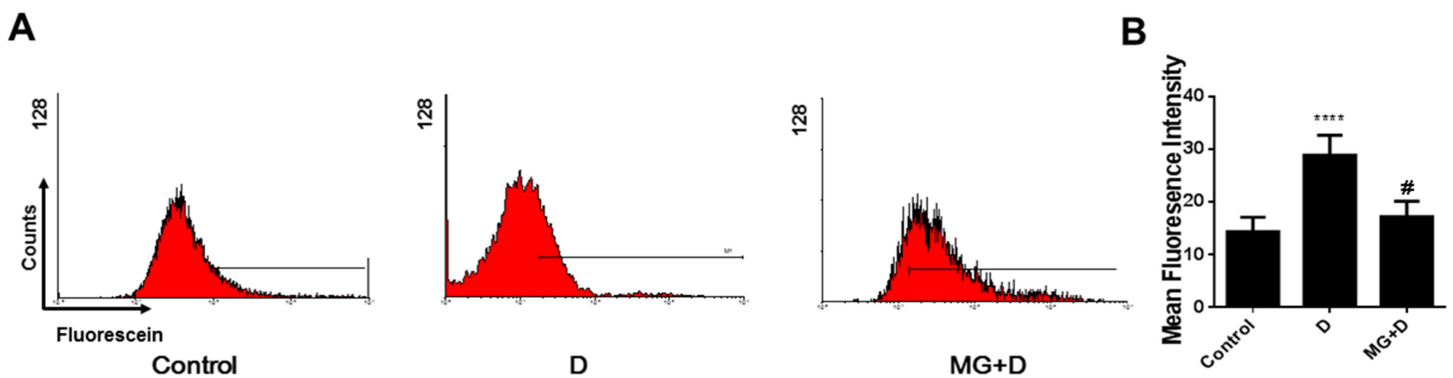

Fig 3. GB pretreatment decreased the level of reactive oxygen species (ROS) in cardiomyocytes treated with DOX. (A) Flow cytometry analysis of ROS level in cardiomyocytes treated with 5 µM GB (MG) before subjection to DOX induced cardiotoxicity. (B) Quantification of the mean fluorescence intensity (MFI) obtained from Flow cytometry. ****$p<0.0001$ when compared to control group, #$p<0.0001$ when compared to DOX.

doi:10.1371/journal.pone.0168219.g003

ROS was involved in the protective effect of GB

The reactive oxygen species (ROS) is reported to be in involved in the DOX-induced cardio-toxicity. To examine whether GB exerts its protective effect through ROS, we performed flow
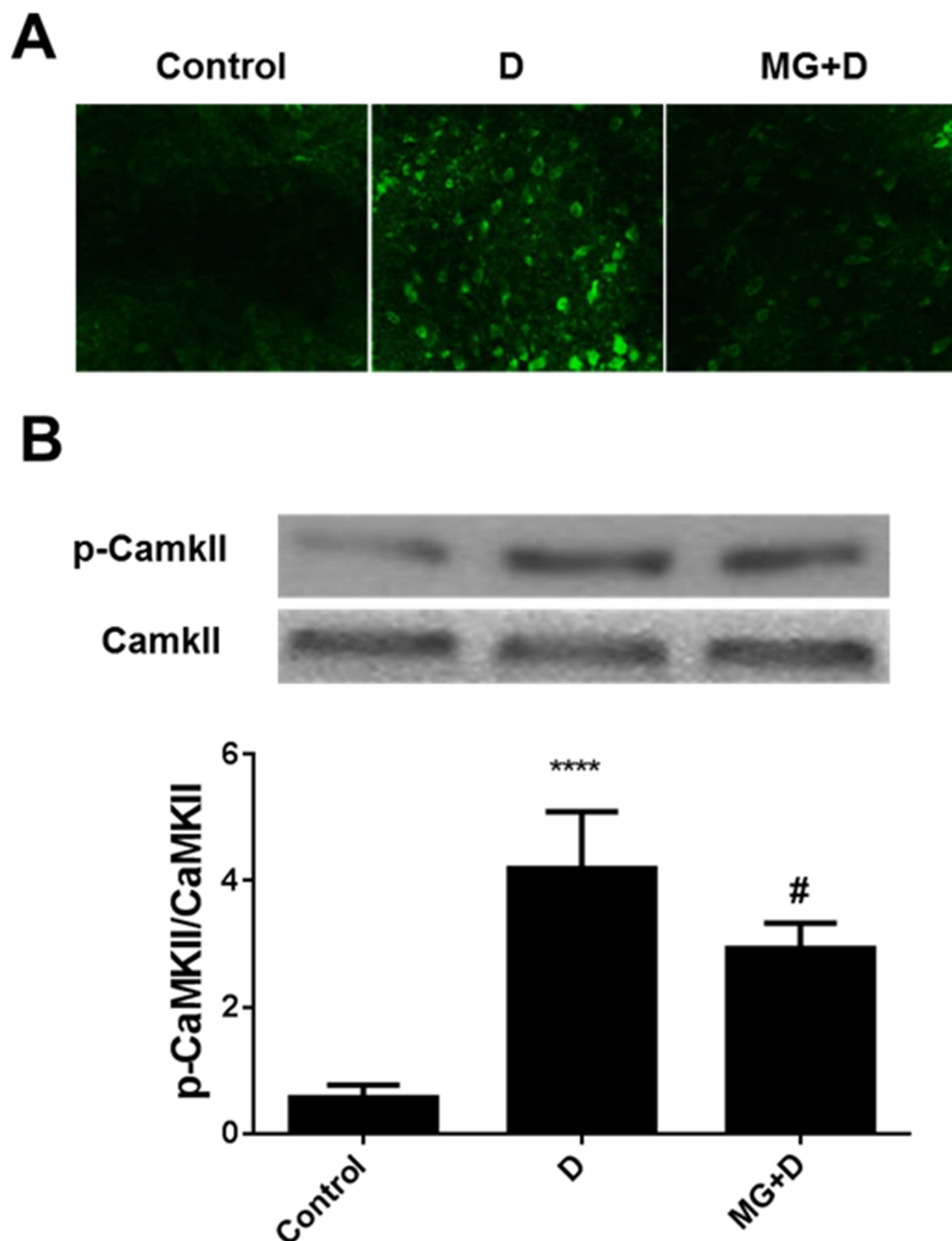

Fig 4. Intracellular calcium level and CaMKII phosphorylation was involved in the protective effect of GB in DOX induced cardiotoxicity. (**A**) Intracellular calcium level was determined by Fura-2/AM probe. Increased intracellular calcium level was found after DOX treatment while GB pretreatment could significantly decrease the calcium level (**B**). Western blot analysis of CaMKII phosphorylation. Increased CaMKII phosphorylation was found after DOX treatment while GB pretreatment could significantly decrease the CaMKII phosphorylation. ****$p<0.0001$ when compared to control group, #$p<0.0001$ when compared to DOX.
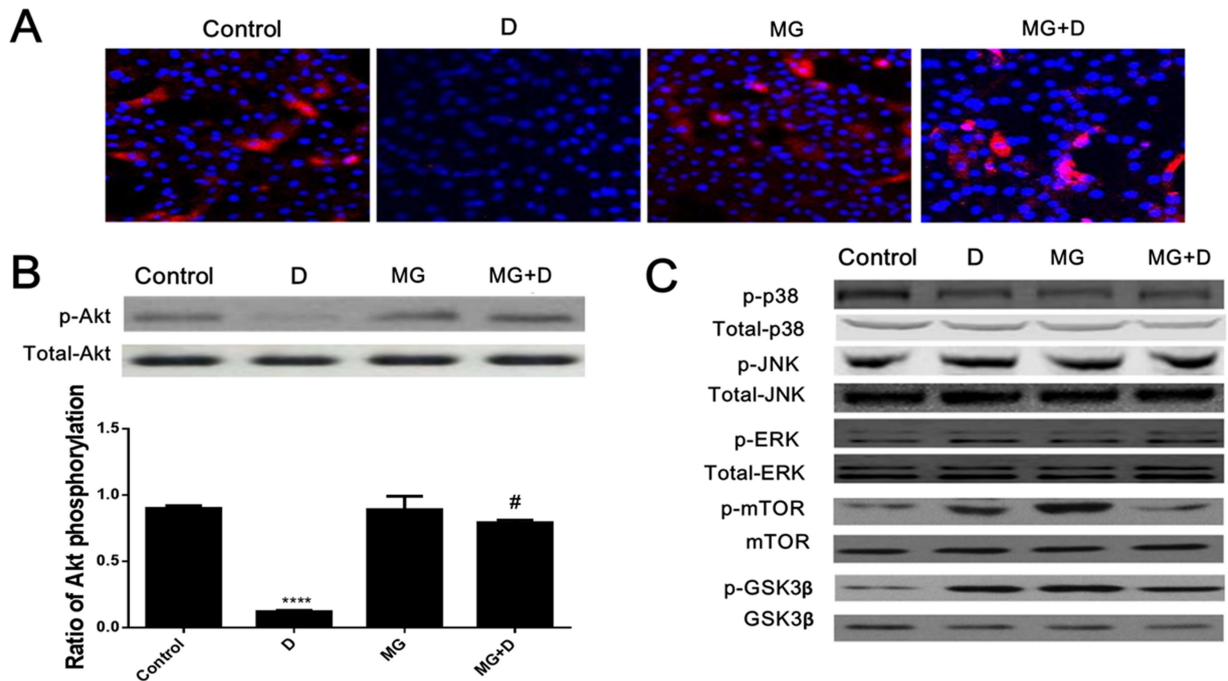
doi:10.1371/journal.pone.0168219.g004

Fig 5. Akt phosphorylation was involved in the protective effect of GB in DOX induced cardiotoxicity. (**A**) Immunofluorescence analysis of Akt phosphorylation. Decreased Akt phosphorylation was found after DOX treatment but pretreatment with GB restored this effect. (**B**) Western-blot analysis of Akt phosphorylation. Significantly decreased Akt phosphorylation was found after DOX treatment but GB treatment significantly activated the Akt phosphorylation. (**C**) Phosphorylation of p38, JNK, Erk, mTOR and GSK3β was not involved in the protective effect of GB in DOX induced cardiotoxicity. No significant difference was found on p38, p-JNK, p-Erk, p-mTOR and p-GSK3β as detected by western-blot analysis. ****$p < 0.0001$ when compared to control group, #$p < 0.0001$ when compared to DOX.

doi:10.1371/journal.pone.0168219.g005

cytometry analysis for determination of ROS levels. The results showed that DOX treatment increased ROS levels while GB pretreatment significantly inhibited ROS expression in DOX-treated mice (Fig 3). These results indicate that GB exerts its protective effects via downregulation of ROS.

Intracellular calcium level and CaMKII phosphorylation was involved in the protective effect of GB pretreatment

Fura-2/AM probe was employed to examine the intracellular calcium level. We observed that GB pretreatment could reverse the DOX-induced upregulation of calcium levels induced by treatment (Fig 4A). Moreover, we observed the effect of GB pretreatment could significantly decrease CaMKII phosphorylation (Fig 4B).

Akt phosphorylation was involved in the protective effect of GB

We further performed the immunofluoresence (Fig 5A) and western-blot analysis (Fig 5B) to assess the role of Akt phosphorylation in the protective effect of GB pretreatment. GB pretreatment could reverse the downregulation of Akt phosphorylation induced by DOX. Moreover, GB pretreatment did not affect the phosphorylation of p38, JNK, Erk, mTOR and GSK-3β (Fig 5C).

Inhibition of CaMKII and Akt pathways protects against DOX-induced cardiotoxicity. Due to the effects of GB on CaMKII and Akt phosphorylation, we aimed to verify if inhibition of these pathways could affect cell viability. Cardiomyocytes were treated with PI3K
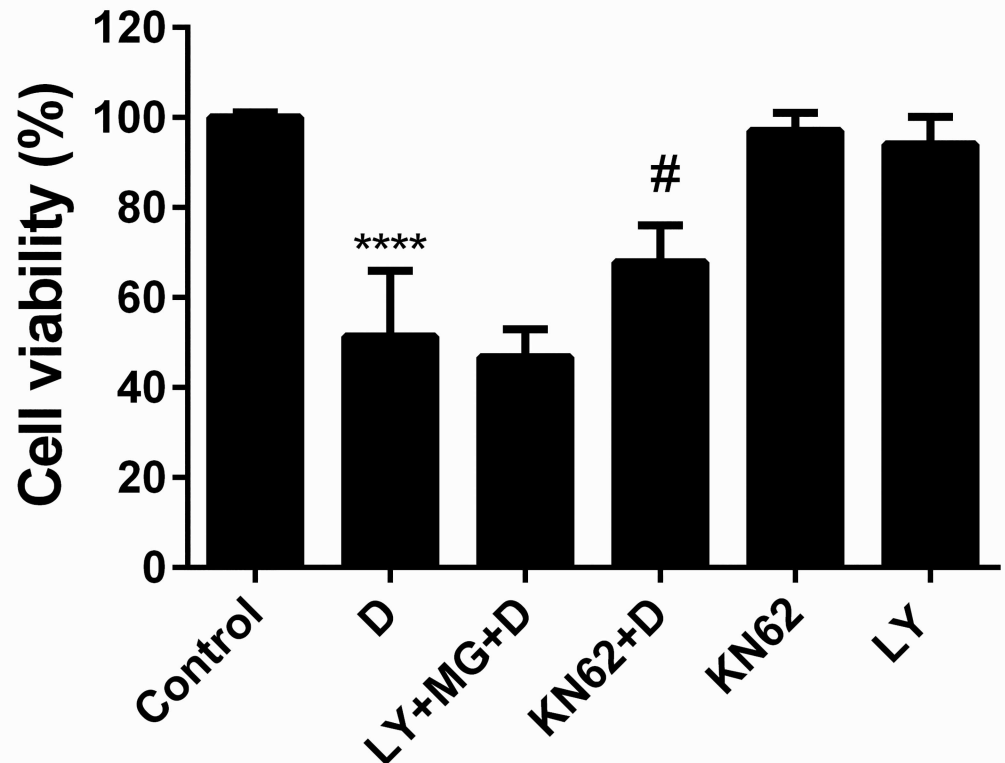
Fig 6. GB exert its protective effect by activating the PI3K/Akt pathway and inhibiting the CaMKII pathway.
Cardiomyocytes cell viability analysis was determined by MTT assay. PI3K inhibitor LY294002 (10 μM)
pretreatment inhibited the protective effect of GB pretreatment in DOX induced cardiotoxicity while CaMKII inhibitor
KN62 (10 μM) pretreatment significantly increased cell viability. ****$p<0.0001$ when compared to control group,
#$p<0.01$ when compared to DOX group.

doi:10.1371/journal.pone.0168219.g006

inhibitor LY294002 and CaMKII inhibitor KN62 and the cell viability measured. The results
showed that PI3K inhibitor LY294002 pretreatment could reverse the protective effect of GB
in DOX-induced cardiotoxicity while CaMKII inhibitor KN62 pretreatment significantly
increased cell viability (Fig 6). These results suggest that GB exert its protective effect by acti-
vating the PI3K/Akt pathway and inhibiting the CaMKII pathway.

Protective effect of GB on cardiac function in DOX induced cardiotoxic model *in vivo*

In the *in vivo* model, no significant difference was found on the mouse weight in mice treated
with DOX, GB or both (Fig 7A). On the contrary, significant improvement of the left ventricle
ejection fraction LVEF and decreased left ventricle mass (LVM) in mice treated with GB in
DOX induced cardiotoxic model (Fig 7B).

Discussion

In the present study, we investigated the protective effects of GB on DOX-induced cardiotoxi-
city and found that GB pretreatment significantly improved cell viability by inhibiting cell
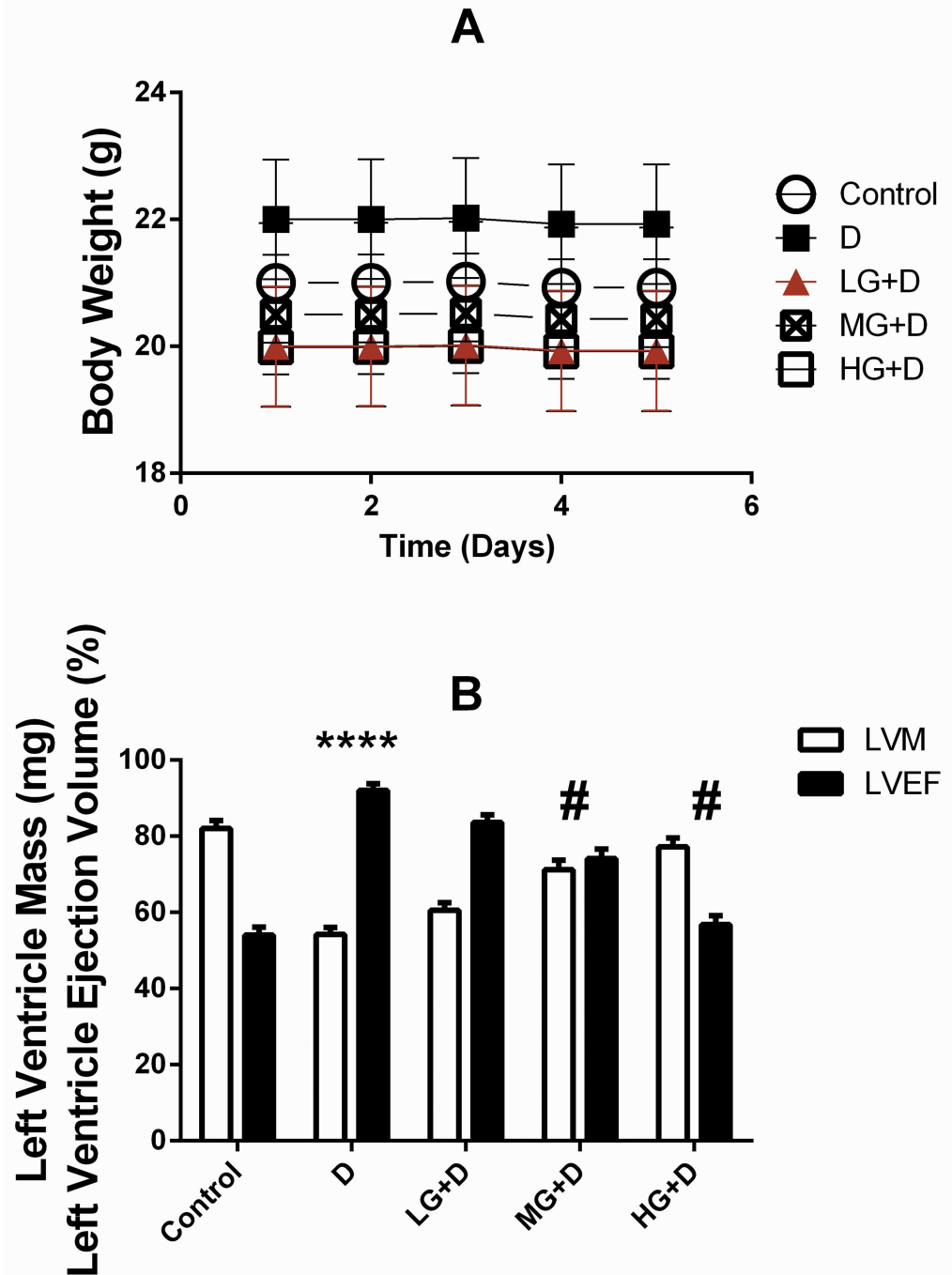
Fig 7. Protective effect of GB on cardiac function in DOX induced cardiotoxic model *in vivo*. (A) No significant difference was recorded regarding mouse weight in mice treated with DOX, GB or both. (B) Significant improvement of the left ventricle ejection fraction (LVEF) and decreased left ventricle mass (LVM) were found in mice treated with GB in DOX-induced cardiotoxic model. ****$p<0.0001$ when compared to control group, #$p<0.05$ when compared to DOX.

doi:10.1371/journal.pone.0168219.g007

apoptosis. We equally found that GB pretreatment decreased ROS and intracellular calcium levels and increased Akt phosphorylation in the cardiotoxic cell model. In the *in vivo* cardiotoxic model, we found improved LVEF and decreased LV mass in the mice treated with GB. To the best of our knowledge, our study is the first to systemically assess the cardioprotective effect of GB against DOX-induced cardiotoxicity *in vitro* and *in vivo*.

Currently, the exact mechanisms about DOX-induced cardiotoxicity remains unclear. However, multiple studies have suggested that oxidative stress plays a critical role in the pathogenesis of DOX induced cardiotoxicity [48–50]. DOX induced cellular damage is mediated by an iron-anthracycline complex formation and this complex has the ability to generate free radicals that could cause severe plasma membrane and cytoskeleton structure damage [51]. Due to the lack of effective antioxidant defense mechanisms, anthracycline-induced reactive oxygen species (ROS) could cause severe injury to the heart and because of the central role of ROS in the mechanism of DOX-induced myocardium damage [52], we here examined the anti-oxidative role of GB against DOX-induced toxicity. We observed that GB pretreatment significantly decreased ROS level, which indicates that the protective function of GB against DOX-induced cardiotoxicity is partly due to its anti-oxidative properties.

When cardiomyocytes are subjected to oxidative stress or ischemia reperfusion, the p38MAPK and PI3K/Akt pathways can be altered inside the cells, leading to apoptotic cell death, which subsequently contribute to the deterioration of cardiac contractile function and left ventricular remodeling. Previous studies have suggested that Akt activation could protect heart function by inhibiting cell apoptosis and p38MAPK inhibition could attenuate cellular inflammatory reactions [53]. Moreover, previous investigations indicated that the activation of PI3K/Akt signaling pathway promotes an essential cell survival signaling in cardiomyocytes [54]. Our present findings showed that GB could reduce DOX-induced cardiac cell death by activating the PI3K/Akt signaling pathway. These results are consistent with previous studies [55–57]. In contrast, we did not observe any significant alteration of P38 expression during the GB pretreatment.

In previous studies on ischemia and ischemia-reperfusion induced cardiac arrhythmia, it was demonstrated that GB is able to exert anti-ischemia and cardioprotective effects by inhibiting the increase of the left ventricular end diastolic pressure, improving post ischemia-reperfusion cardiac pump function and protecting the ischemia myocardium from calcium overload reaction due to its negative effect on the intracellular calcium level [58, 59]. Herein, in conformity with the above studies, we equally discovered that GB could decrease the intracellular calcium level and protect from the myocardium damage induced by DOX treatment. Moreover, as previously shown in a mouse model of cardiotoxicity [60], we observed that GB could significantly improve the LVEF and LV mass, thus indicating the substantial effectiveness of GB pretreatment for the body.

Conclusion

In conclusion, GB exhibits protective effects against DOX-induced cardiotoxicity *in vitro* and *in vivo* by modulating ROS, Akt and calcium pathways. The present findings will contribute in the heart protection during DOX chemotherapy.

Acknowledgments

Author Contributions

Conceptualization: JG TC ZL.

Data curation: JG TC DZ JZ ZL.

Formal analysis: JG TC DZ JZ.

Funding acquisition: JZ ZL.

Investigation: JG TC DZ JZ.

Methodology: JG TC DZ.

Project administration: JG TC DZ JZ ZL.

Resources: JG TC DZ JZ ZL.

Software: DZ JZ.

Supervision: JG TC DZ JZ ZL.

Validation: JG TC DZ JZ ZL.

Visualization: JG JZ ZL.

Writing – original draft: JG ZL.

Writing – review & editing: JG TC DZ JZ ZL.

References

1. Lv S, Li M, Tang Z, Song W, Sun H, Liu H, et al. Doxorubicin-loaded amphiphilic polypeptide-based nanoparticles as an efficient drug delivery system for cancer therapy. Acta biomaterialia. 2013; 9 (12):9330–42. doi: 10.1016/j.actbio.2013.08.015 PMID: 23958784

2. Xu C, Tian H, Wang P, Wang Y, Chen X. The suppression of metastatic lung cancer by pulmonary administration of polymer nanoparticles for co-delivery of doxorubicin and Survivin siRNA. Biomaterials science. 2016; 4(11):1646–54. Epub 2016/10/19. doi: 10.1039/c6bm00601a PMID: 27709139

3. Fernandes RS, Silva JO, Monteiro LO, Leite EA, Cassali GD, Rubello D, et al. Doxorubicin-loaded nanocarriers: A comparative study of liposome and nanostructured lipid carrier as alternatives for cancer therapy. Biomedicine & pharmacotherapy = Biomedecine & pharmacotherapie. 2016; 84:252–7. Epub 2016/10/22.

4. Pallerla S, Gauthier T, Sable R, Jois SD. Design of a doxorubicin-peptidomimetic conjugate that targets HER2-positive cancer cells. European journal of medicinal chemistry. 2016; 125:914–24. Epub 2016/10/22. doi: 10.1016/j.ejmech.2016.10.015 PMID: 27769032

5. Dias QC, Nunes ID, Garcia PV, Favaro WJ. Potential therapeutic strategies for non—muscle invasive bladder cancer based on association of intravesical immunotherapy with p—mapa and systemic administration of cisplatin and doxorubicin. International braz j urol: official journal of the Brazilian Society of Urology. 2016; 42(5):942–54. Epub 2016/10/21.

6. Baghbani F, Moztarzadeh F, Mohandesi JA, Yazdian F, Mokhtari-Dizaji M. Novel alginate-stabilized doxorubicin-loaded nanodroplets for ultrasounic theranosis of breast cancer. International journal of biological macromolecules. 2016; 93(Pt A):512–9. Epub 2016/10/23. doi: 10.1016/j.ijbiomac.2016.09.008 PMID: 27601134

7. Varshosaz J, Hassanzadeh F, Aliabadi HS, Khoraskani FR, Mirian M, Behdadfar B. Targeted delivery of doxorubicin to breast cancer cells by magnetic LHRH chitosan bioconjugated nanoparticles. International journal of biological macromolecules. 2016; 93(Pt A):1192–205. Epub 2016/10/23. doi: 10.1016/j.ijbiomac.2016.07.025 PMID: 27693338

8. Xiang S, Dauchy RT, Hauch A, Mao L, Yuan L, Wren MA, et al. Doxorubicin resistance in breast cancer is driven by light at night-induced disruption of the circadian melatonin signal. Journal of pineal research. 2015; 59(1):60–9. Epub 2015/04/11. PubMed Central PMCID: PMCPMC4490975. doi: 10.1111/jpi.12239 PMID: 25857269

9.   Xin Z, Jiang S, Jiang P, Yan X, Fan C, Di S, et al. Melatonin as a treatment for gastrointestinal cancer: a review. Journal of pineal research. 2015; 58(4):375–87. Epub 2015/03/11. doi: 10.1111/jpi.12227 PMID: 25752643

10. Chan BY, Hughes BG, Roczkowsky A, de Souza P, Armanious G, Young HS, et al. Myocardial Matrix Metalloproteinase-2 Activation Impairs Amplitude and Frequency of Spontaneous Intracellular Ca2+ Transients in Doxorubicin Cardiotoxicity. The FASEB Journal. 2016; 30(1 Supplement):742.6–.6.

11. Tahover E, Patil YP, Gabizon AA. Emerging delivery systems to reduce doxorubicin cardiotoxicity and improve therapeutic index: focus on liposomes. Anti-cancer drugs. 2015; 26(3):241–58. doi: 10.1097/CAD.0000000000000182 PMID: 25415656

12. Wang J, Zhang X, Feng C, Sun T, Wang K, Wang Y, et al. MicroRNA-532-3p regulates mitochondrial fission through targeting apoptosis repressor with caspase recruitment domain in doxorubicin cardio-toxicity. Cell death & disease. 2015; 6(3):e1677.

13. Kumar S, Marfatia R, Tannenbaum S, Yang C, Avelar E. Doxorubicin-induced cardiomyopathy 17 years after chemotherapy. Texas Heart Institute Journal. 2012; 39(3).

14. Govender J, Loos B, Marais E, Engelbrecht AM. Mitochondrial catastrophe during doxorubicin-induced cardiotoxicity: a review of the protective role of melatonin. Journal of pineal research. 2014; 57(4):367–80. Epub 2014/09/19. doi: 10.1111/jpi.12176 PMID: 25230823

15. Yang Y, Sun Y, Yi W, Li Y, Fan C, Xin Z, et al. A review of melatonin as a suitable antioxidant against myocardial ischemia-reperfusion injury and clinical heart diseases. Journal of pineal research. 2014; 57 (4):357–66. Epub 2014/09/19. doi: 10.1111/jpi.12175 PMID: 25230580

16. Ponnusamy L, Mahalingaiah PS, Singh KP. Chronic oxidative stress increases resistance in renal carci-noma cells to doxorubicin-induced cytotoxicity potentially through epigenetic mechanism. Cancer Research. 2015; 75(15 Supplement):4571–.

17. Zhang S, Liu X, Bawa-Khalfe T, Lu L-S, Lyu YL, Liu LF, et al. Identification of the molecular basis of doxorubicin-induced cardiotoxicity. Nature medicine. 2012; 18(11):1639–42. doi: 10.1038/nm.2919 PMID: 23104132

18. Carvalho FS, Burgeiro A, Garcia R, Moreno AJ, Carvalho RA, Oliveira PJ. Doxorubicin-Induced Cardio-toxicity: From Bioenergetic Failure and Cell Death to Cardiomyopathy. Medicinal research reviews. 2014; 34(1):106–35. doi: 10.1002/med.21280 PMID: 23494977

19. Dong Q, Chen L, Lu Q, Sharma S, Li L, Morimoto S, et al. Quercetin attenuates doxorubicin cardiotoxi-city by modulating Bmi-1 expression. British Journal of Pharmacology. 2014; 171(19):4440–54. doi: 10.1111/bph.12795 PMID: 24902966

20. Durham K, Trigatti B. Scavenger Receptor Class B Type I Is Required for Protection by High-Density Lipoprotein Against Doxorubicin-Induced Apoptosis in Both Mouse and Human Cardiomyocytes and Cardiotoxicity in Mice. Arteriosclerosis, Thrombosis, and Vascular Biology. 2014; 34(Suppl 1):A428–A.

21. Ludke A, Sharma AK, Bagchi AK, Singal PK. Subcellular basis of vitamin C protection against doxorubi-cin-induced changes in rat cardiomyocytes. Molecular and cellular biochemistry. 2012; 360(1–2):215–24. doi: 10.1007/s11010-011-1059-z PMID: 21938406

22. Hao E, Mukhopadhyay P, Cao Z, Erdélyi K, Holovac E, Liaudet L, et al. Cannabidiol Protects against Doxorubicin-Induced Cardiomyopathy by Modulating Mitochondrial Function and Biogenesis. Molecular medicine. 2015; 21(1).

23. Jay SM, Murthy AC, Hawkins JF, Wortzel JR, Steinhauser ML, Alvarez LM, et al. An engineered biva-lent neuregulin protects against doxorubicin-induced cardiotoxicity with reduced proneoplastic potential. Circulation. 2013; 128(2):152–61. doi: 10.1161/CIRCULATIONAHA.113.002203 PMID: 23757312

24. Sin TK, Tam BT, Yung BY, Yip SP, Chan LW, Wong CS, et al. Resveratrol protects against doxorubi-cin-induced cardiotoxicity in aged hearts through the SIRT1-USP7 axis. The Journal of physiology. 2015; 593(8):1887–99. doi: 10.1113/jphysiol.2014.270101 PMID: 25665036

25. Asensio-López MC, Sánchez-Más J, Pascual-Figal DA, Abenza S, Pérez-Martínez MT, Valdés M, et al. Involvement of ferritin heavy chain in the preventive effect of metformin against doxorubicin-induced cardiotoxicity. Free Radical Biology and Medicine. 2013; 57:188–200. doi: 10.1016/j.freeradbiomed.2012.09.009 PMID: 23000260

26. Sun J, Sun G, Meng X, Wang H, Luo Y, Qin M, et al. Isorhamnetin protects against doxorubicin-induced cardiotoxicity in vivo and in vitro. PloS one. 2013; 8(5):e64526. doi: 10.1371/journal.pone.0064526 PMID: 23724057

27. Jagetia GC, Reddy TK. The grape fruit flavonone naringin protects mice against doxorubicin-induced cardiotoxicity. Journal of Molecular Biochemistry. 2014; 3(1).

28. Swarnakar NK, Thanki K, Jain S. Enhanced antitumor efficacy and counterfeited cardiotoxicity of combi-natorial oral therapy using Doxorubicin-and Coenzyme Q10-liquid crystalline nanoparticles in

comparison with intravenous Adriamycin. Nanomedicine: Nanotechnology, Biology and Medicine. 2014; 10(6):1231–41.

29. Swarnakar NK, Thanki K, Jain S. Bicontinuous cubic liquid crystalline nanoparticles for oral delivery of Doxorubicin: implications on bioavailability, therapeutic efficacy, and cardiotoxicity. Pharmaceutical research. 2014; 31(5):1219–38. doi: 10.1007/s11095-013-1244-8 PMID: 24218223

30. Wang Z, Zhang J, Ren T, Dong Z. Targeted metabolomic profiling of cardioprotective effect of Ginkgo biloba L. extract on myocardial ischemia in rats. Phytomedicine. 2016; 23(6):621–31. doi: 10.1016/j.phymed.2016.03.005 PMID: 27161403

31. Baliutyte G, Baniene R, Gendviliene V, Martisiene I, Trumbeckaite S, Borutaite V, et al. Influence of ethanol extract of Ginkgo biloba leaves on the isolated rat heart work and mitochondria functions. Journal of cardiovascular pharmacology. 2012; 59(5):450–7. doi: 10.1097/FJC.0b013e318249171d PMID: 22240914

32. Khan MA, Singh M, Khan MS, Ahmad W, Najmi AK, Ahmad S. Alternative approach for mitigation of doxorubicin-induced cardiotoxicity using herbal agents. Current clinical pharmacology. 2014; 9(3):288–97. PMID: 23342982

33. Huang C-H, Yang M-L, Tsai C-H, Li Y-C, Lin Y-J, Kuan Y-H. Ginkgo biloba leaves extract (EGb 761) attenuates lipopolysaccharide-induced acute lung injury via inhibition of oxidative stress and NF-κB-dependent matrix metalloproteinase-9 pathway. Phytomedicine. 2013; 20(3):303–9.

34. Parimoo HA, Sharma R, Patil RD, Sharma OP, Kumar P, Kumar N. Hepatoprotective effect of Ginkgo biloba leaf extract on lantadenes-induced hepatotoxicity in guinea pigs. Toxicon. 2014; 81:1–12. doi: 10.1016/j.toxicon.2014.01.013 PMID: 24472344

35. Escárcega-González CE, Reynoso-Andeola IG, Jaramillo-Juárez F, Martínez-Ruvalcaba H, Posadas del Rio FA. The Ginkgo biloba Extract Reverses the Renal Effects of Titanium Dioxide Nanoparticles in Adult Male Rats. Biochemistry research international. 2016; 2016.

36. Yang Y, Nemoto EM, Harvey SA, Subbotin VM, Gandhi CR. Increased hepatic platelet activating factor (PAF) and PAF receptors in carbon tetrachloride induced liver cirrhosis. Gut. 2004; 53(6):877–83. Epub 2004/05/13. PubMed Central PMCID: PMC1774060. doi: 10.1136/gut.2003.024893 PMID: 15138217

37. Xia SH, Hu CX, Fang JM, Di Y, Zhao ZL, Liu LR. G[alpha]i2 and G[alpha]q expression change in pancreatic tissues and BN52021 effects in rats with severe acute pancreatitis. Pancreas. 2008; 37(2):170–5. Epub 2008/07/31. doi: 10.1097/MPA.0b013e3181661b07 PMID: 18665079

38. Mahmoud F, Abul H, Onadeko B, Khadadah M, Haines D, Morgan G. In vitro effects of Ginkgolide B on lymphocyte activation in atopic asthma: comparison with cyclosporin A. Jpn J Pharmacol. 2000; 83 (3):241–5. Epub 2000/08/22. PMID: 10952073

39. Kaur N, Dhiman M, Perez-Polo JR, Mantha AK. Ginkgolide B revamps neuroprotective role of apurinic/apyrimidinic endonuclease 1 and mitochondrial oxidative phosphorylation against Abeta25-35 -induced neurotoxicity in human neuroblastoma cells. Journal of neuroscience research. 2015; 93(6):938–47. doi: 10.1002/jnr.23565 PMID: 25677400

40. Yu L, Liang H, Dong X, Zhao G, Jin Z, Zhai M, et al. Reduced silent information regulator 1 signaling exacerbates myocardial ischemia-reperfusion injury in type 2 diabetic rats and the protective effect of melatonin. Journal of pineal research. 2015; 59(3):376–90. Epub 2015/09/04. doi: 10.1111/jpi.12269 PMID: 26327197

41. Yu L, Liang H, Lu Z, Zhao G, Zhai M, Yang Y, et al. Membrane receptor-dependent Notch1/Hes1 activation by melatonin protects against myocardial ischemia-reperfusion injury: in vivo and in vitro studies. Journal of pineal research. 2015; 59(4):420–33. Epub 2015/08/27. doi: 10.1111/jpi.12272 PMID: 26308963

42. Chen X, Li X, Du Z, Shi W, Yao Y, Wang C, et al. Melatonin promotes the acquisition of neural identity through extracellular-signal-regulated kinases 1/2 activation. Journal of pineal research. 2014; 57 (2):168–76. Epub 2014/06/20. doi: 10.1111/jpi.12153 PMID: 24942200

43. Yuan W, Guo J, Li X, Zou Z, Chen G, Sun J, et al. Hydrogen peroxide induces the activation of the phospholipase C-gamma1 survival pathway in PC12 cells: protective role in apoptosis. Acta biochimica et biophysica Sinica. 2009; 41(8):625–30. Epub 2009/08/07. PMID: 19657563

44. Spallarossa P, Altieri P, Garibaldi S, Ghigliotti G, Barisione C, Manca V, et al. Matrix metalloproteinase-2 and -9 are induced differently by doxorubicin in H9c2 cells: The role of MAP kinases and NAD(P)H oxidase. Cardiovasc Res. 2006; 69(3):736–45. Epub 2005/10/11. doi: 10.1016/j.cardiores.2005.08.009 PMID: 16213474

45. Nozaki N, Shishido T, Takeishi Y, Kubota I. Modulation of doxorubicin-induced cardiac dysfunction in toll-like receptor-2-knockout mice. Circulation. 2004; 110(18):2869–74. Epub 2004/10/27. doi: 10.1161/01.CIR.0000146889.46519.27 PMID: 15505089

46. Guenancia C, Li N, Hachet O, Rigal E, Cottin Y, Dutartre P, et al. Paradoxically, iron overload does not potentiate doxorubicin-induced cardiotoxicity in vitro in cardiomyocytes and in vivo in mice. Toxicology

and applied pharmacology. 2015; 284(2):152–62. Epub 2015/02/26. doi: 10.1016/j.taap.2015.02.015 PMID: 25711856

47.   He B, Zhao Y, Xu L, Gao L, Su Y, Lin N, et al. The nuclear melatonin receptor RORalpha is a novel endogenous defender against myocardial ischemia/reperfusion injury. Journal of pineal research. 2016; 60(3):313–26. Epub 2016/01/23. doi: 10.1111/jpi.12312 PMID: 26797926

48.   Ghibu S, Delemasure S, Richard C, Guilland JC, Martin L, Gambert S, et al. General oxidative stress during doxorubicin-induced cardiotoxicity in rats: absence of cardioprotection and low antioxidant efficiency of alpha-lipoic acid. Biochimie. 2012; 94(4):932–9. Epub 2011/03/15. doi: 10.1016/j.biochi.2011.02.015 PMID: 21396425

49.   Yu X, Cui L, Zhang Z, Zhao Q, Li S. alpha-Linolenic acid attenuates doxorubicin-induced cardiotoxicity in rats through suppression of oxidative stress and apoptosis. Acta biochimica et biophysica Sinica. 2013; 45(10):817–26. Epub 2013/07/31. doi: 10.1093/abbs/gmt082 PMID: 23896563

50.   Granados-Principal S, El-Azem N, Pamplona R, Ramirez-Tortosa C, Pulido-Moran M, Vera-Ramirez L, et al. Hydroxytyrosol ameliorates oxidative stress and mitochondrial dysfunction in doxorubicin-induced cardiotoxicity in rats with breast cancer. Biochemical pharmacology. 2014; 90(1):25–33. Epub 2014/04/15. doi: 10.1016/j.bcp.2014.04.001 PMID: 24727461

51.   Iqbal M, Dubey K, Anwer T, Ashish A, Pillai KK. Protective effects of telmisartan against acute doxorubicin-induced cardiotoxicity in rats. Pharmacological reports: PR. 2008; 60(3):382–90. Epub 2008/07/16. PMID: 18622063

52.   Potemski P, Polakowski P, Wiktorowska-Owczarek AK, Owczarek J, Pluzanska A, Orszulak-Michalak D. Amifostine improves hemodynamic parameters in doxorubicin-pretreated rabbits. Pharmacological reports: PR. 2006; 58(6):966–72. Epub 2007/01/16. PMID: 17220557

53.   Chaanine AH, Hajjar RJ. AKT signalling in the failing heart. European journal of heart failure. 2011; 13 (8):825–9. Epub 2011/07/05. PubMed Central PMCID: PMC3143831. doi: 10.1093/eurjhf/hfr080 PMID: 21724622

54.   Walsh K. Akt signaling and growth of the heart. Circulation. 2006; 113(17):2032–4. Epub 2006/05/03. doi: 10.1161/CIRCULATIONAHA.106.615138 PMID: 16651482

55.   Cao Y, Ruan Y, Shen T, Huang X, Li M, Yu W, et al. Astragalus polysaccharide suppresses doxorubicin-induced cardiotoxicity by regulating the PI3k/Akt and p38MAPK pathways. Oxidative medicine and cellular longevity. 2014; 2014:674219. Epub 2014/11/12. PubMed Central PMCID: PMC4216718. doi: 10.1155/2014/674219 PMID: 25386226

56.   Chen YL, Zhuang XD, Xu ZW, Lu LH, Guo HL, Wu WK, et al. Higenamine Combined with [6]-Gingerol Suppresses Doxorubicin-Triggered Oxidative Stress and Apoptosis in Cardiomyocytes via Upregulation of PI3K/Akt Pathway. Evidence-based complementary and alternative medicine: eCAM. 2013;2013:970490. Epub 2013/07/19. PubMed Central PMCID: PMC3687593.

57.   Swain SM, Whaley FS, Ewer MS. Congestive heart failure in patients treated with doxorubicin: a retrospective analysis of three trials. Cancer. 2003; 97(11):2869–79. Epub 2003/05/27. doi: 10.1002/cncr.11407 PMID: 12767102

58.   Zhang ZX, Qi XY, Xu YQ. [Effect of ginkgolide B on L-type calcium current and cytosolic [Ca2+]i in guinea pig ischemic ventricular myocytes]. Sheng li xue bao: [Acta physiologica Sinica]. 2003; 55 (1):24–8. Epub 2003/02/25.

59.   Qi XY, Zhang ZX, Xu YQ. Effects of Ginkgolide B on action potential and calcium, potassium current in guinea pig ventricular myocytes. Acta pharmacologica Sinica. 2004; 25(2):203–7. Epub 2004/02/11. PMID: 14769210

60.   Lamberti M, Giovane G, Garzillo EM, Avino F, Feola A, Porto S, et al. Animal models in studies of cardiotoxicity side effects from antiblastic drugs in patients and occupational exposed workers. BioMed research international. 2014; 2014:240642. PubMed Central PMCID: PMC3950409. doi: 10.1155/2014/240642 PMID: 24701565